APL Materials

Research Update: Large-area deposition, coating, printing, and processing techniques for the upscaling of perovskite solar cell technology

Cite as: APL Mater. 4, 091508 (2016); https://doi.org/10.1063/1.4962478
Submitted: 27 June 2016 • Accepted: 24 August 2016 • Published Online: 19 September 2016

Stefano Razza, Sergio Castro-Hermosa, Aldo Di Carlo, et al.

Research Update: Large-area deposition, coating, printing, and processing techniques for the upscaling of perovskite solar cell technology

Stefano Razza,[a] Sergio Castro-Hermosa,[a] Aldo Di Carlo, and Thomas M. Brown[b]
CHOSE - Centre for Hybrid and Organic Solar Energy, Department of Electronic Engineering, University of Rome Tor Vergata, Via del Politecnico 1, 00133 Rome, Italy

(Received 27 June 2016; accepted 24 August 2016; published online 19 September 2016)

To bring perovskite solar cells to the industrial world, performance must be maintained at the photovoltaic module scale. Here we present large-area manufacturing and processing options applicable to large-area cells and modules. Printing and coating techniques, such as blade coating, slot-die coating, spray coating, screen printing, inkjet printing, and gravure printing (as alternatives to spin coating), as well as vacuum or vapor based deposition and laser patterning techniques are being developed for an effective scale-up of the technology. The latter also enables the manufacture of solar modules on flexible substrates, an option beneficial for many applications and for roll-to-roll production. [http://dx.doi.org/10.1063/1.4962478]

INTRODUCTION

The ability to achieve high power conversion efficiencies (PCE) over large area modules is an important characteristic for a photovoltaic (PV) technology with industrial aspirations. Generally, increasing the geometrical dimensions of a PV device brings up new different issues with respect to those related to small area solar cells. Low cost manufacturing of Perovskite Solar Cells (PSCs) requires new evolutions in techniques previously developed for other thin film technologies like Dye Solar Cells (DSCs) and polymer solar cells.[1–3] For example, the knowledge accrued on TiO_2 as electron transport layer and on molecular compounds as hole transport material (HTM) has been important in the development of PSCs. However, PSCs are based on a completely different light absorbing material, composed of perovskite crystals which form layers which are difficult to control morphologically especially over large areas. Crystallization occurs during solvent evaporation, which is strictly related to the deposition technique as well as substrate surface used. The roughness of the layer is influenced by the manufacturing process and each technique requires its own settings for film optimization and to avoid the presence of pin-holes or other inhomogenieties. Some of the techniques used for small area cells are not applicable to large areas, either because of their complexity or because large amounts of material are wasted. Some parts of the materials used, like perovskite precursors and their solvents, are toxic, so manufacturing must take into consideration the safety of the processes. Apart from the charge transport and perovskite layers, the device architectures incorporate metals (usually the top contact) the deposition of which is also associated with issues. In fact, a PSC is composed of several layers with different chemical compositions and the corrosion or formation of complexes induced by chemical interactions must also be taken into consideration. Currently, most of the high efficiency PSCs reported in the literature use gold as top electrode, since the presence of iodide inside the perovskite film limits the possibility of using silver or other metals which can lead to poor stability.[4] Recently, carbon pastes have been utilized instead

[a]S. Razza and S. Castro-Hermosa contributed equally to this work.
[b]Author to whom correspondence should be addressed. Electronic mail: thomas.brown@uniroma2.it

of the top metal electrode which can also be printed over large areas.[5,6] Generally thin film solar cells use conductive glass or plastic films as substrate photo-electrodes. The required transparency limits the conductivity, generating problems in terms of series resistance when increasing device dimensions. High series resistances lead to low fill factors reducing the efficiency. To reduce this problem, it is possible to use metal grids to collect the current (typically used for traditional silicon solar modules) or make modules composed of series-connected sub-cells to limit currents (the most common configuration for thin film technologies). In order to reduce the length charges, need to move, cells are made rectangular, with their geometry optimized as a function of current density and sheet resistance of the electrodes. Before PSCs, layout optimization was developed for DSC and OPV modules.[7–9] Modules based on series connections ensure low currents (and high voltages), but they require high uniformity and reproducibility over the module area because low performance output of even one cell will decrease the efficiency of the entire module.[8] To find the optimal dimensions for large area PSCs Galagan and co-workers studied the relationship between active area size and PCE.[10] They supported their experimental results with a theoretical DC simulation, with a particular focus on the substrates sheet resistance, in order to find a good match between transparency and substrate sheet resistance. The study of the optimal width for modules sub-cells is also related to the space required for each connection between cells. Cells with a reduced width have a low series resistance and consequently a better fill factor, but reducing the width means an increase in the number of connections, losing active area across the substrate. This is why high resolution patterning, with techniques such as raster laser systems, is implemented to maintain efficiencies over aperture areas.[11] Apart from vacuum processing[12–14] which plays an important role for deposition of the two electrodes, and can also be employed for depositing the transport and perovskite layers, a characteristic feature of perovskite solar cell technology is that of determining the two dimensional shape or patterns of one or more of its constituent layers over large substrate areas by utilizing, together with laser processing, methods adopted from both printing and coating industry. The quality and uniformity achieved for the layers, with typical thicknesses between 100 nm and 300 nm, is critical for the scale up process of this technology. Here we will cover some of the developments carried out for effective module manufacturing via the study and the optimization of some of the main low-cost large-area processing techniques that have been employed for this purpose.

SPIN COATING

High uniformity represents one of the main objectives for the scale-up process of the various layers. For small area solar cells, the deposition technique that is used most is spin coating. An important aspect of spin coating is the high thickness and film quality control that can be obtained by setting speed, time, and acceleration of the sample rotation together with ink formulation. High levels of reproducibility and good uniformity are accomplished. It is generally via spin coating (of the main constituent layers) that the highest efficiencies have been reported over small laboratory cells (typical dimensions of ~0.1 cm^2) with the record being 22.1%.[15] However, it must be noted that tests on larger cells, i.e., ≥1 cm^2, are more appropriate for gauging performance figures and limits for a PV technology. For example, when passing from cells of 0.1 cm^2 area to 1 cm^2 area, the drop in efficiency can be contained to within ~10%-15% in relative terms.[16,17] Via a solvent-solvent extraction approach with excess methylammonium (MA) iodide in the precursor solution Yang *et al.*[17] achieved a PCE of 16.3% with a stabilized output of 15.6% in $CH_3NH_3PbI_3$ perovskite based cells on an area of 1.2 cm^2. The efficiency in planar glass/FTO/NiMgLiO/$CH_3NH_3PbI_3$/PCBM/Ti(Nb)O_x/Ag cells, prepared by spin coating by Chen *et al.*, was 16.2% over an area of 1.02 cm^2 and hysteresis was negligible, i.e., within 0.3% in absolute PCE values. In 2015 the certified efficiency record over an area of ≥1 cm^2 was held by Japan's National Institute for Materials Science for a perovskite solar cell of 1.02 cm^2 with a PCE of 15.6% (initial, not stabilised).[18] In 2016, Li *et al.*,[19] obtained shiny, smooth, and crystalline mixed $FA_{0.81}MA_{0.15}PbI_{2.51}Br_{0.45}$ perovskite films containing formamidium (FA) and Br by a simple vacuum-flash solution processing method where the spin-coated film was placed for a few seconds into a vacuum chamber (optimal results were achieved at a pressure of 20 Pa) to boost solvent

removal and rapid crystallization before thermal annealing at 100 °C for 30 min. Cells with an active area of 1.44 cm^2 measured using a black mask with an aperture area of 1.0×1.0 cm^2 delivered a maximum efficiency of 20.5% and a certified PCE of 19.6%.

Although ~1 cm^2 areas are larger than most small laboratory cell reports, the areas that need to be considered when developing mini or large scale modules are at least an order of magnitude larger. The first paper in the literature reporting perovskite modules and how their efficiency varied with dimension (see Figure 1(a)) was indeed based on spin coating of the main active layers, achieving a PCE of 5.1% over module active area.[20] The modules were obtained by the series connection of 5 sub-cells (Figure 1(b)). Also using a spin coated perovskite layer, Qiu *et al.*[21] realized a module with four series-connected cells with a PCE of 13.6% over an aperture area of 4 cm^2. Figure 1(c) shows the device with its structure analysed by a cross-section SEM. Devices also presented small hysteresis in the I-V curves because of the improvement of morphology and crystallinity of perovskite layer. Large grains and a pinhole-free layer were obtained as a result of the use of a new precursor mixture ($Pb(CH_3CO_2)_2 \cdot 3H_2O$, $PbCl_2$, and $CH_3NH_3PbI_3$) which induced a fast crystallization. Matteocci *et al.*[22] fabricated perovskite based modules over larger dimensions, reaching an aperture area PCE of 9.1% (13.0% on active area) for a device active area above 10 cm^2. To study the uniformity of the module's electrical output, IPCE maps were graphed (Figure 1(d)), giving important information on uniformity and on the local currents over the module's area. Spin coating ensures flexibility in adopting either the one step process (i.e., using one ink made of a mixture of the two precursors) or the sequential step deposition (e.g., lead iodide first and then methylammonium iodide) for forming polycrystalline perovskite films.[22] Heo *et al.*,[23] fabricated an inverted planar-structured

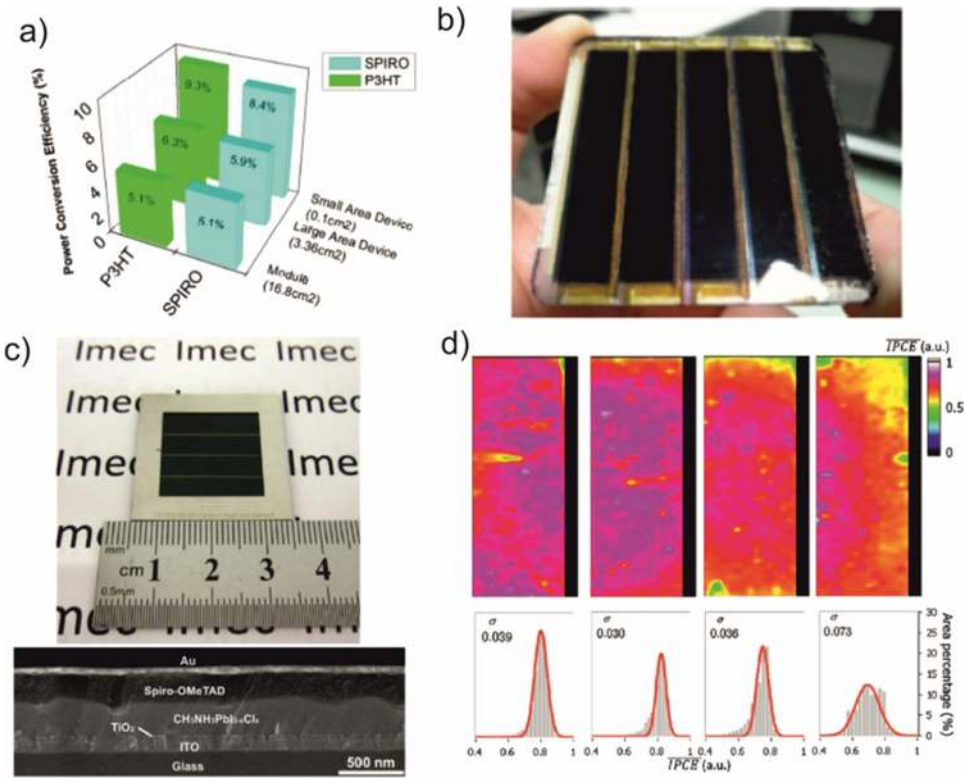

FIG. 1. (a) PCE evolution for different size perovskite devices fabricated using P3HT and Spiro-OMeTad as HTM. (b) Image of spin coated perovskite based module with 16 cm^2 active area. Reproduced with permission from Matteocci *et al.*, Phys. Chem. Chem. Phys. **16**, 3918 (2014). Copyright 2014 Royal Society of Chemistry. (c) Perovskite based module composed of series connection of 4 sub-cells with a PCE up to 13.6% and a cross-section SEM of device structure. Reproduced with permission from Qiu *et al.*, Energy Environ. Sci. **9**, 484 (2016). Copyright 2016 Royal Society of Chemistry. (d): IPCE map of 10 cm^2 perovskite module. Reproduced with permission from Matteocci *et al.*, Prog. Photovoltaics Res. Appl. **24**, 436 (2014). Copyright 2014 John Wiley and Sons.

(ITO/PEDOT:PSS/CH_3NH_3PbI3/PCBM/Au) solar module with an active area of 40 cm^2 and a PCE of 12.9% (over the active area). Although the authors did not report hysteresis effects on the module, tests carried out on small cells showed negligible hysteresis in the I-V curves which was mainly linked to the good balance between electron and hole flux and a small concentration of crystalline defects.[23] Although efficiencies achieved with spin coating have been high, ensuring good levels of reproducibility and thickness and morphology control, the sizes of the module have been relatively small and the technique does not really represent an effective solution for the scale up of perovskite solar cell manufacturing. A large percentage of the ink volume is wasted during the spin coating process, leading to a substantial increase in costs and exposure to potentially harmful chemicals. Alternative deposition techniques have been developed that can minimize these drawbacks and are more apt for large scale fabrication and will be described in the sections titled "Blade coating"–"Conclusions".

BLADE COATING

One of the printing techniques that can represent a simple and cheap option for large area processing is represented by blade coating. For example, lead iodide precursor can be deposited by blade coating over the conducting substrate, as the first step in the sequential deposition of perovskite.[24] Generally, the blade coating applicator has a simple setting system consisting of a micrometre screw, the turning of which makes it possible to adjust the height of the blade from the substrate surface. Furthermore, blade coating allows one to adopt different strategies to control layer thickness and morphology and is very cheap to implement. The perovskite crystal size is influenced by the substrate temperature and by the deposition time, so the control of solvent evaporation rate is mandatory to get a good quality final layer. The solvent evaporation rate of the deposited inks can be controlled by several ways: by heating the substrates even up to the boiling point of the solvent used, or by applying an air flow over the surface during the coating procedure. Mallajosyula *et al.*[25] reported deposition of perovskite layers by one-step blade coating over large area substrates. The perovskite formed large islands whose size was determined by the volume of the solution (mixture of PbI_2 + MACl in dimethylformamide (DMF) with 1:1 of molar ratio) and substrate temperature. Perovskite islands with large size led to hysteresis-free behaviour in solar devices and a PCE of 7.32% (active area of 1 cm^2). In 2015 Razza *et al.* implemented an air assisted process to deposit lead iodide perovskite precursor in order to achieve uniform large area deposition.[26] Perovskite and its precursors can be dissolved in few solvents, generally toxic, like N,N-Dimethylformamide (DMF), Dimethyl Sulfoxide (DMSO), or Gamma-Butyrolactone (GBL), so the use of a technique which requires a low amount of solution represents a clear benefit. Modules with a PCE of 10.4% over 10 cm^2 active area and 4.3% over 100 cm^2 (Figure 2(a)) were realized using a sequential step process to transform a blade coated lead iodide layer into a perovskite layer. Optimizing the Spiro-OMeTAD deposition by blade coating the same group achieved 9% efficiency over 100 cm^2 active area.[27] Blade coating was also used to fabricate planar heterojunction PSCs, showing a best PCE of 12.2% and good stability in air.[28] Note that blade coating is a cheap and scalable technique and can be used to deposit not only the perovskite active layer but also HTMs and ETL layers, leading to fully printable devices as demonstrated by Yang *et al.* on both glass and flexible substrates.[29] In order to increase reproducibility and automation of deposition it is possible to use the slot die coating, a technique based on a similar principle, but with the possibility of controlling the amount of ink used more precisely and of obtaining a patterned layout.

SLOT DIE COATING

One of the most promising printing techniques for the scale up of PSC manufacturing is slot-die coating. Vak *et al.* used it to print a lead iodide layer as the first step in the sequential step synthesis of perovskite films.[30] A continuous nitrogen flow over the surface during deposition helped ensure film uniformity, control the solvent evaporation rate and prevent pin-hole formation. As previously reported for blade coating, control of solvent evaporation during and/or after deposition is required to obtain good layer morphology. The same paper showed a slot-die head fabricated

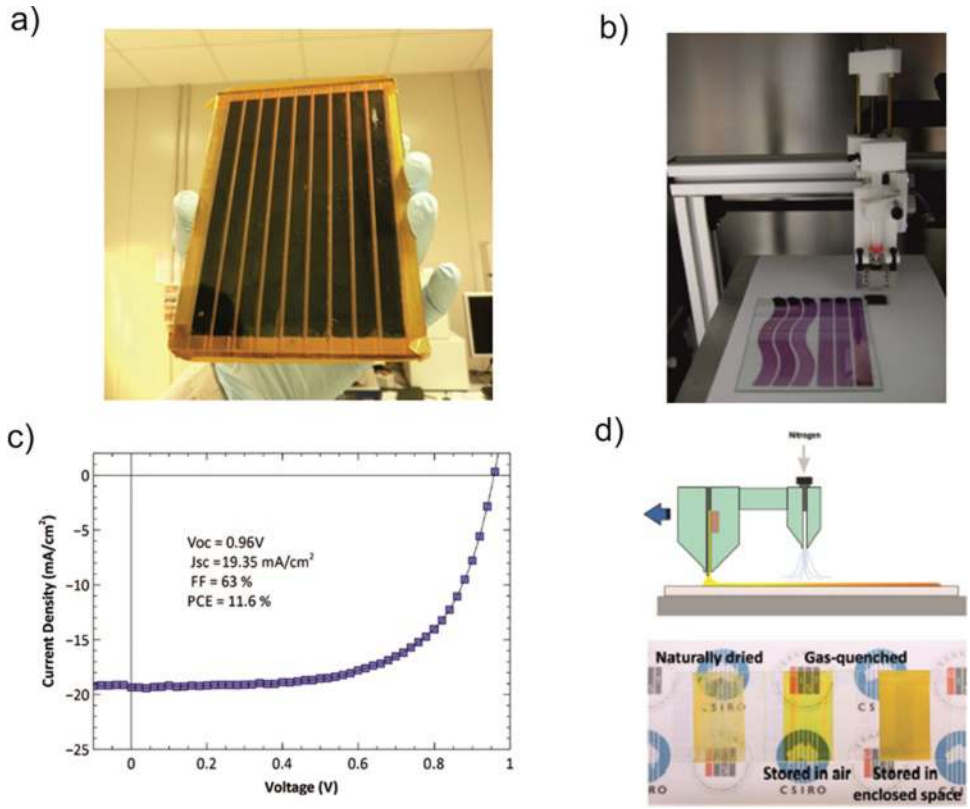

FIG. 2. (a) 100 cm^2 active area module based on blade coated Perovskite layer. Reproduced with permission from Razza *et al.*, J. Power Sources, **277**, 286 (2015). Copyright 2015 Elsevier. (b) Slot-die coater with different layout deposition. (c) J-V curve of a solar cell (active area = 0.1 cm^2) based on slot-die perovskite deposition. Reproduced with permission from Vak *et al.*, Adv. Energy Mater. **5**, 1 (2015). Copyright 2015 John Wiley and Sons. (d) PbI_2 deposition by slot-die coating with different gas quenching strategies. Reproduced with permission from Hwang *et al.*, Adv. Mater. **27**, 1241 (2015). Copyright 2015 John Wiley and Sons.

with a 3D printer (Figure 2(b)). Perovskite solar cells fabricated in this way exhibited a PCE of 11% (Figure 2(c)), but the most important result in terms of scale up was the 47.3 cm^2 active area of the module, which delivered a PCE of 4.57%. A further confirmation of the appropriateness of slot-die for PSC fabrication came from Hwang *et al.*[31] who showed in more detail the influence of gas drying during lead iodide deposition (Figure 2(d)). Slot die coating can also replace the second step of the sequential process which is usually that of dip coating the whole substrate in a methylammonium iodide solution, used to form the final perovskite film. It was possible to control the crystallization temperature with advantages in terms of reproducibility and morphology control. The cells showed different efficiencies under various processing temperatures with a maximum PCE of 11.96% at a temperature of 70 °C, which represents a very encouraging result for cells composed of all printed layers (except for the electrodes).[31] Solliance recently reported a module with a PCE of 10% on an aperture area of 168 cm^2 using industrial scalable slot die coating in combination with laser patterning.[32] Slot-die is a promising printing technique to improve the scale up of perovskite solar cell fabrication, and can be particularly important even for roll to roll manufacturing. In the paragraph covering flexible PSCs, we will in fact describe more developments related to slot die coating on this matter.

SPRAY COATING

Another industrial coating technique used to obtain high quality thin layers over large area substrates is spray deposition.[33] The manufacture of solar cells with spray-coated perovskite layers[34]

with efficiencies of up to 11% in single step deposition was made possible by the optimization of processing parameters like substrate temperature, gas carrier, and annealing treatments.[35] PSCs fabricated with the spin coating process were still used as reference devices. Figure 3(a) shows a comparison between spray coated and spin coated perovskite cells. The PCE and SEM images obtained (Figures 3(a) and 3(b)) prove the possibility of obtaining efficient solar cells with spray coating of the perovskite layer. A perovskite film with high uniformity, crystallinity, and surface coverage was obtained in a single step with a resulting cell PCE of 13% by Sanjib *et al.*[36] with ultrasonic spray-coating. This, combined with optical curing of TiO_x layers, led to flexible perovskite cells on polyethylene terephthalate (PET) substrates with a PCE equal to 8.2%. Although these results were not obtained on large area substrates, the small hysteresis observed in the I-V curves (attributed to use of the planar device architecture) and the significant PCEs reached show that spray coating can be potentially scaled up to large areas. Further studies should concentrate on the effectiveness, uniformity, etc., of spray coating over very large areas. Pin-hole free and low roughness films are mandatory to obtain high efficiency perovskite solar cells. Several studies in the literature show how methylammonium iodide vapour as a second step over PbI_2 films can create a smooth perovskite layer as an alternative to dip-coating.[12,14,37] An alternative option as a second step consists in spray coating the methylammonium iodide solution over the lead iodide layer[38,39] (see Figure 3(c)).[40] A comparison between perovskite layers obtained by dip-coating and spray coating of the methylammonium solution revealed a better morphology for the spray coated sample (Figures 3(d) and 3(e))[40] and PCEs of up to 14.3% achieved.[41] Spray coating is also useful to deposit other materials that can be introduced into perovskite device structures. Whereas spray coating of graphene ink was demonstrated in DSCs,[42] a spray coated solution of

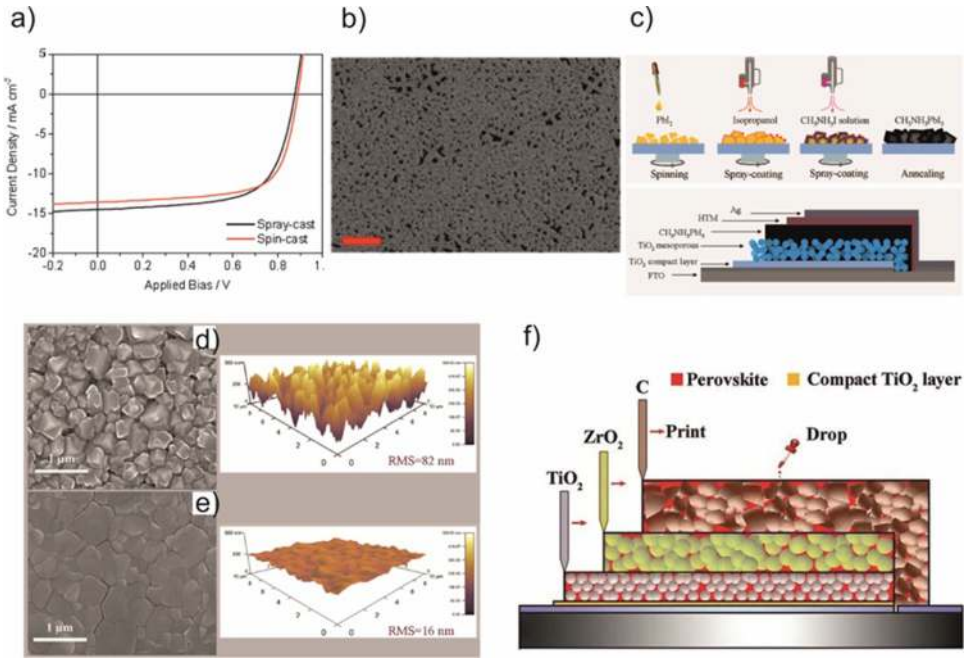

FIG. 3. (a) Average current-density versus voltage characteristics for spray coated and spin coated perovskite solar cells. (b) SEM image of a spray coated perovskite layer ($CH3NH3PbI_{3-x}Cl_x$) on PEDOT:PSS. Reproduced with permission from Barrows *et al.*, Energy Environ. Sci. **7**, 1 (2014). Copyright 2014 Royal Society of Chemistry. (c) Scheme of perovskite crystallization process made by spray coating of methylammonium solution and final perovskite cell architecture. (d) SEM top view image and AFM topography of perovskite layer obtained by traditional dipping process. (e) SEM top view image and AFM topography of perovskite layer obtained by spray coating methylammonium solution process, with a very low roughness. Reproduced with permission from Li *et al.*, Mater. Lett. **157**, 38 (2015). Copyright 2015 Elsevier. (f) Architecture of the fully printed mesoscopic perovskite solar cell where the mesoporous triple layer stack of TiO_2, ZrO_2, and carbon black/graphite top electrode was deposited by screen printing before infiltration of the perovskite. Reproduced with permission from Mei *et al.*, Science. **345**, 295 (2014). Copyright 2014 The American Association for the Advancement of Science.

reduced graphene oxide was used as HTM in perovskite solar cells by Palma *et al.* obtaining longer device shelf life compared to an organic HTM.[43] Another application of spray coating is to deposit alternatives to transparent conducting oxides (TCOs) such as a highly conductive poly (3,4-ethylenedioxythiophene):poly(styrenesulfonate) PEDOT:PSS films, which were incorporated as semitransparent anodes in highly flexible TCO-free perovskite solar cells.[44]

SCREEN PRINTING

Screen printing is a technique that adopts a screen made of a synthetic fibre or steel mesh onto which a pattern is drawn with an emulsion. By squeegee pressure one is able to transfer pastes onto the substrate through the openings in the patterned mesh. Whereas techniques such as slot die coating had been widely adopted in OPV before being utilized in PSCs, screen printing derives mainly from the field of DSCs. In fact, similarly to DSCs, it is mainly utilized for the deposition of the nanocrystalline scaffolds in the mesoporous PSC architectures at both the cell level and module level (since it enables patterned deposition of the unit cells[45]). Arguably one of the most interesting developments regarding screen printing has been the development of fully printed PSCs utilizing a stack of mesoporous layers,[5,46,47] as shown in Figure 3(f).[48] A three-layer stack of 1 μm mesoporous TiO_2 ETL, a 2 μm mesoporous ZrO_2 spacer layer, and a 10 μm mesoporous carbon black/graphite top electrode were all screen printed over a conducting substrate covered by a thin compact layer of TiO_2. The cell was completed by infiltrating the perovskite through the carbon electrode filling the whole triple layer mesoporous stack delivering an efficiency of 12.8% and remarkable stability over 1000 h of full sunlight.[48] The specified thicknesses ($\geq$1 μm) are those typically seen in screen printed layers even though thicknesses down to a few hundred nms can be achieved (the very thin compact layer, $\leq$100 nm, is typically still deposited via other techniques such as spray pyrolysis[48] or ALD[45]) as demonstrated in the quadruple stacks by Cao *et al.*[49] There, an additional 800 nm mesoporous nickel oxide interlayer was screen printed just underneath the 10 μm carbon black/graphite to improve charge collection and reduce charge recombination resulting in a PCE of 15%. A similar architecture (and PCE) had been fabricated by Xu *et al.* via blade coating the layers.[50] Solaronix[99] developed an 8-cell module with a quadruple screen-printed stack, including the compact blocking layer, in a glass/FTO/c-TiO_2(~50 nm)/meso-TiO_2(~0.5 μm)/meso-ZrO_2(~1 μm)/porous-carbon(~15 μm) configuration with a PCE of 9.9% over 47.6 cm^2 active area (PCE = 12% on a 1 cm^2 cell) with good stability. The $CH_3NH_3PbI_3$ perovskite was infiltrated in the stack by drop-casting the solution on the active surface followed by drying at ~50 °C for 24h. The full printability and low cost of the whole layer stack including the carbon paste electrode, and its associated stability, make this approach a promising one for the up-scaling of the technology.

LASER PATTERNING

Coating techniques such as spin coating or blade coating are not self-patterned. One can use masks and/or chemical etching to create the required layout, but often precluding uniform deposition of materials when doing so. Furthermore, the use of thermoplastic masks is not possible when combined with strong solvents and/or high temperatures, and the application of metallic masks is not easy.[22] Furthermore, every time a new geometrical layout is required a new mask would have to be prepared. This can be a cumbersome process. The ability to precisely change the pattern (either for performance or aesthetical evaluation) is not only very useful for prototyping and development but also for manufacturing. The prime post-patterning process for perovskite solar cells is represented by laser processing as detailed in the review by Mincuzzi *et al.*[11] A perovskite solar cell is composed of several layers with a thickness of a few hundred nanometers. Laser processing aims to pattern each layer avoiding damage to the underlying layers or TCO substrate. Laser systems can be used to remove parts of the previously deposited layers for contacting in order to obtain high quality (inter) connections. Using different laser wavelengths, it is possible to remove several materials, layer by layer or all at once. The choice is related to the different deposition techniques used.[26] Matteocci *et al.* showed how module efficiency could be increased up to 13% by using laser processes, instead of solvents, to remove the material in excess whilst keeping clean the contact areas and thus

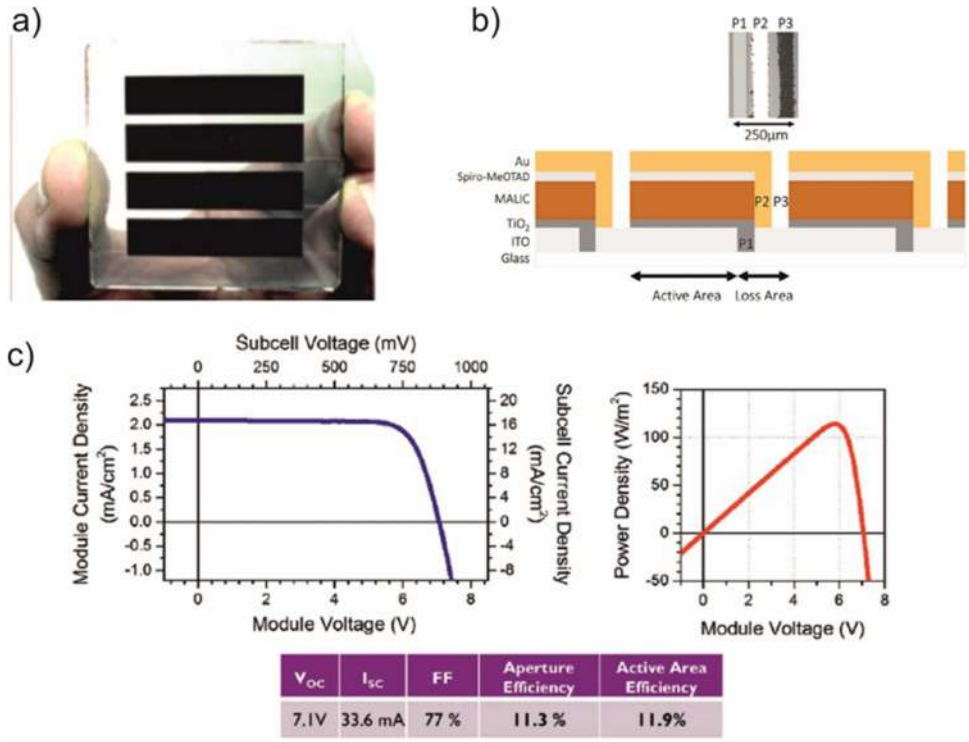

FIG. 4. (a) Laser patterned perovskite and Spiro-OMeTad layers for module fabrication as described in Ref. 22. (b) Patterning scheme for P1-P2-P3 scribing with minimized loss area for high aperture ratio modules. (c) Electrical parameters of 16 cm^2 module and sub-cells. Reproduced with permission from Gehlhaar *et al.*, SPIE Newsroom (29 October 2015). Copyright 2015 SPIE (The international society for optics and photonics).

ensuring low resistance connections over module area (Figure 4(a)).[22] Whereas most layers have been ablated by working on the laser wavelengths and parameters, for particularly difficult layers to remove, such as TiO_2 nano-rods, an intermediate thin compact layer of TiO_2 between the TCO and the mesoporous nanorod layer was shown to facilitate the patterning of the latter without damaging the TCO.[51,52] The presence of a TiO_2 scaffold, compared to modules without (i.e., planar), led to improved device stability.[51] Patterning and shaping by means of lasers brings many advantages such as a very high precision, resolution, processing speed, automation, high selectivity, and low cost.[11] Laser patterning is able to reduce the dead areas in perovskite based modules, minimizing such areas used for contacts.[53] Patterning can be performed in three sequential steps (P1-P2-P3) used to create the necessary spacing/isolation for the electrodes of adjacent sub cells (P1-P3) and to isolate clean the contact areas (P3). Figure 4(b) shows the scribes and their role in cell connections. This strategy, obtained by laser ablation (for P1) and mechanical scribing (for P2, P3), led to a module with a PCE over active area of up to 11.9% (Figure 4(c)), with a loss in area equal to only 5% of aperture area.[54] Mechanical scribing may be replaced with full laser scribing. A remarkable result was obtained also by the application of laser patterning to flexible modules, with a geometrical aperture ratio of up to 92.5%.[55] At the moment one of the best efficiencies for a perovskite based module is 13.6% over aperture area.[20] In this work the P1-P2-P3 patterning procedures played an important role, improving the aperture ratio up to 91%.

ROLL-TO-ROLL COMPATIBLE DEPOSITION

Those printing techniques that are compatible with Roll-to-Roll (R2R) processing reproducibly[30,31,56] present huge potential in being able to produce large scale, low-cost flexible devices with high throughput.[31,57] R2R has been implemented successfully already in solar cell manufacturing, especially in the field of organic solar cells[58–60] and even DSCs.[61] Although many groups have used

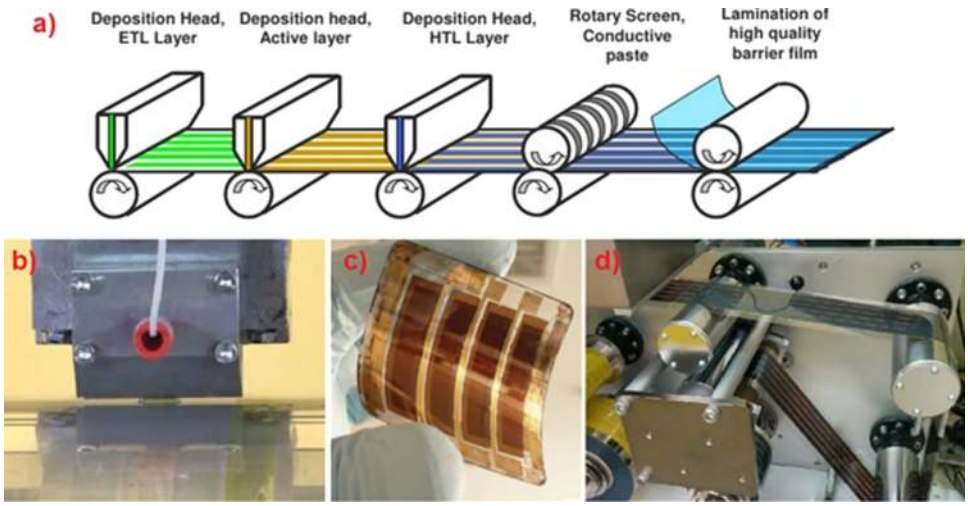

FIG. 5. (a) An example of a schematic of inline roll-to-roll manufacturing process for organic solar modules which is transferable also to perovskite solar cell fabrication: ETL, active and HTL layers are deposited by slot-die technique whereas the back electrode is screen printed before lamination of a barrier film. Reproduced with permission from V. Shrotriya, Solarmer, Printed Electronics USA 15, 2010, http//www.slideshare.net/vshrotriya/organic-Solar-Cells. Copyright 2010 Shrotriya, Solarmer. Photographs of: (b) PbI_2 layer deposited by slot-die process. Reproduced with permission from Schmidt *et al.*, Adv. Energy Mater. **5**, 1500569 (2015). Copyright 2015 John Wiley and Sons; (c) flexible perovskite solar module, reproduced with permission from Di Giacomo *et al.*, Adv. Energy Mater. **5**, 1401808 (2015). Copyright 2015 John Wiley and Sons; and (d) roll-to-roll production of perovskite solar cells by slot-die. Reproduced with permission from Hwang *et al.*, Adv. Mater. **27**, 1241 (2015). Copyright 2015 John Wiley and Sons.

R2R-compatible printing techniques on glass including slot-die,[30,31] inkjet,[62] and blade coating,[26] the deposition parameters (coating speed, flow rate, temperature, drying, materials)[56,63] must be optimized newly when depositing on flexible substrates. Hwang *et al.*[31] optimized ETL, perovskite, and HTL printed deposition through slot-die on PET/ITO substrates with a vacuum evaporated Ag back electrode. At the moment, Schmidt *et al.*[64] are the first group to develop a fully printed flexible perovskite solar cell starting from PET/ITO, including the top contact, together with encapsulation.

Figure 5(a) shows the schematic design of general R2R manufacturing line to process organic solar cells[65] which is adaptable to the manufacture of the planar perovskite solar cell structure (PET/ITO/ETL/perovskite/HTL/back electrode).[30,31,64] In this kind of R2R design, the PET/ITO substrate is constantly unwinding and passing underneath the manufacturing units where deposition and encapsulation processes take place. Finally, the full device is rewound on the second roll. For ETL, active and HTL layer R2R deposition, slot-die has been selected as arguably the most suitable technique.[30,31,63,64] Slot-die coating of the PbI_2 stripe is shown in Figure 5(b). Slot-die coatings are highly uniform,[31,63] their layer width ranges from a few millimetres[66] to centimetres[63,67] depending on the design[30,31,56,63] and their layer thickness can be determined by controlling the deposition speed and flow.[30,31,56,60,64,68] Whereas the ETL layers of ZnO have reported thickness down to 23 nm,[64] the perovskite layer thickness was approximately 300 nm.[31] Finally, the back electrode can be made through rotary screen printing as well as R2R vacuum techniques for metal deposition and a barrier film can be laminated over the solar cell to improve stability.[59,60,64]

LARGE AREA FLEXIBLE DEVICES

Several authors have developed flexible perovskite solar cells as described in a recent review.[69] However, most of these works have been carried out on small cell areas and/or based on spin coating or other techniques that are considered incompatible with large scale manufacturing. Di Giacomo *et al.*[45] fabricated the first flexible perovskite solar module. The four series-connected structures (see Figure 5(c)) incorporated a mesoporous scaffold (i.e., PET/ITO/TiO_2_CL/TiO_2-scaffold/perovskite/Spiro-OMeTAD/Au) and delivered a PCE of 3.1%. Fabrication of the module

was enabled by screen printing of the mesoporous TiO_2 in rectangular strips and laser patterning of masks. Ultrathin (11 nm) TiO_2 compact layers via atomic layer deposition and UV-irradiated mesoporous TiO_2 scaffolds (which improved stability of unencapsulated devices compared to those with no scaffolds) enabled the processing to occur at low temperatures compatible with the PET substrates.

Whereas the perovskite and HTL layers in the above work were deposited via spin coating, R2R fully printed flexible perovskite solar cells in which all the active layers, ETL, perovskite, and HTL deposition were carried out using slot-die coating have been reported with the back electrode being either evaporated[31] or screen printed.[64] For their flexible device (PET/ITO/ZnO/perovskite/P3HT/Ag), Hwang *et al.*[31] found that layer drying is a critical factor in the transition from spin coating to slot die. ETL and HTL deposition was optimized implementing a flow of N_2 for drying. The perovskite layer was produced by two step sequential slot-die deposition. First, a layer of PbI_2 was coated and gas-dried. Then it was covered with methylammonium iodide. Substrate temperature during deposition of the latter affected the morphology of the final perovskite layer. Films coated at room temperature exhibited small-size crystals, while films at 70 °C showed larger 1 μm-size cubic-shaped crystals. Additionally, device efficiency improved when methylammonium iodide concentration was increased to 40 mg/ml compared to when lower concentrations were used. Over small cells (10 mm^2 active area) the process led to a PCE of 10.14% on glass substrates. The authors indicated that the continued optimization of the fully R2R printing process shown in Figure 5(d) on plastic substrates is still underway. Schmidt *et al.*[64] studied the difference between inverted and normal geometry, one-step and two-step perovskite deposition, and the optimization of the printed back electrode. Results for devices with active area 0.2–0.5 cm^2 with a PCE of 4.9% showed that an inverted structure (PET/ITO/ZnO/PCBM/perovskite/P3HT/PEDOT:PSS/Ag) was better for printing electrodes compared to the direct geometry (PET/ITO/PEDOT:PSS/perovskite/PCBM/ZnO/Ag). The drop in PCE of PET-based devices compared with those on glass in one-step deposition was mainly due to the effects of the substrate itself while in a two-step process it was mainly due to the change (spin vs. slot die) in coating technique.

INK-JET PRINTING, VACUUM/VAPOR DEPOSITION AND OTHER LARGE AREA FABRICATION TECHNIQUES

In addition to deposition techniques mentioned above, several authors have used other methods such as CVD, or inkjet, flexographic or gravure printing in the fabrication of perovskite solar cells. A table summarizing some of the main deposition techniques[70] is reported in Table I. The good results obtained with some of these techniques at the cell level can be considered promising for when the same will be applied to fabricating modules (rather than cells). Inkjet printing is a non-contact printing technique where ink drops can be deposited on a substrate on demand[71] and has been used to cast the perovskite, ETL, HTL, and electrode layers by different authors.[62,71–74] Layers exhibited homogenous thickness, reproducibility, and controllable size and shape layer area. Wei *et al.*[62] fabricated a perovskite solar cell incorporating a nanocarbon hole-extraction layer via inkjet printing technique for the first time. Ink-jet printing a mixed ink composed of carbon black and CH_3NH_3I (methylammonium iodide, MAI) over the previously spin-coated PbI_2 layer, they managed to achieve simultaneous formation of the perovskite layer and the carbon electrode resulting in a solar cell with a PCE of 11.60% (0.1 cm^2). This simultaneous process reduced recombination effects at the interface between the perovskite layer and nano-carbon electrode producing also I-V curves with small hysteresis. Li *et al.*[72] manufactured a mesostructured perovskite solar cell using a mixture of MAI, PbI_2, and MACl with a molar ratio of 1-x:1:x (x = 0 ~ 0.9) dissolved in γ- butyrolactone (35 wt.%). The latter was selected for its high boiling point which prevented clogging of the print-head. Heating of the substrate during the printing process and the amount of CH_3NH_3Cl used were found to be critical parameters affecting morphology of the perovskite (grain size and uniformity) and consequently of device performance. The best PCE (12.3%) was achieved when heating the substrate at 50 °C and with a MACl ratio of x = 0.6. Bag *et al.*[73] deposited formamidium iodide (FAI) and MAI solutions dissolved in isopropanol (40 mg ml^{-1})) on spin-coated PbI_2 layers using a multi-head inkjet printer. The latter allowed the sequential or simultaneous

TABLE I. Comparison of different large area deposition techniques for fabrication of perovskite solar modules. R2R compatibility, material waste, and layer thickness accuracy values[96–98] columns reproduced/adapted with permission from Y. Galagan and R. Andriesse, in Third Gener. Photovoltaics, edited by V. Fthenakis (InTech, 2012), Chap. 3. Copyright 2012 Intechopen. The "Layer" column indicates which layers have been deposited by the technique in perovskite solar cells. Examples of module PCE showing either high efficiency and/or large area capabilities where at least one of the perovskite precursors was deposited with the deposition technique indicated.

Fabrication technique	R2R compatibility	Material waste	Layer thickness accuracy (nm scale)	Layer	Examples of module PCE with perovskite deposition	Reference
Spin coating[a]	–	Very high	Very good	ETL, HTL, perovskite, electrode	13.6% (4 cm^2) 12.9% (40 cm^2) 3.1% (8 cm^2)[b]	21 23 45
Blade coating	+	Moderate	Good	ETL, HTL, perovskite	10.4% (10 cm^2) 4.3% (100 cm^2)[c]	26 26
Slot die coating	+	Low	Very good	ETL, HTL, perovskite	4.57% (47.3 cm^2) 10% (168 cm^2)[d]	30 32
Spray coating	+	Low/Moderate/ High depending on substrate area and spray system	Low	ETL, HTL, perovskite, electrode	For perovskite deposition only reported on cells	
Screen printing	+	Low	Moderate	ETL, HTL, perovskite, electrode	13% (10 cm^2) in modules with screen printed meso-TiO_2 (spin-coated perovskite). 9.9% (47.6 cm^2) in modules with quadruple stack of screen printed c-TiO_2, meso-TiO_2, meso-ZrO_2, porous-carbon (infiltrated with perovskite).	22 99
Vapour deposition	+	Low	Very good	ETL, HTL, perovskite, electrode	12.2% (64 cm^2)	86
Inkjet printing	+	Low	Good	ETL, HTL, perovskite, electrode	Only reported on cells	
Flexographic printing	+	Low	Moderate	Electrode	Only reported on electrodes	
Gravure printing	+	Low	Good	Perovskite, electrode	Only reported on cells	
New methods	+	Low	Good	Perovskite, electrode	Only reported on cells or for non-perovskite layers	
Lamination	+	Low	Low	Electrode	Only reported on electrodes	

[a]The highest certified PCE for a cell with area of ≥1 cm^2 is 19.6% and was achieved by placing a spin-coated perovskite precursor film in vacuum for a few seconds before annealing.[19]
[b]Flexible module. Module was mainly fabricated by spin coating; however, mesoscopic TiO_2 was screen printed and compact TiO_2 deposited by ALD.
[c]The largest perovskite module reported in journal publication.
[d]As press release.

deposition of the cation solutions. The best PCE (11.1%) was obtained with a MAI:FAI ratio of 2:1. Ink jet printing has been extensively used in organic electronics including the printing of silver grid electrodes in ITO-free polymer solar modules.[71] Similar procedures can be applied to perovskite

solar modules in the future. Another printing method that has been used in the organic solar cell field[75] and has been started to be applied to the perovskite field is gravure printing. Micro-gravure printing and doctor blading were used by Hu *et al.*[76] to produce highly oriented and large-area perovskite nanowires (PNWs) which were used in photodetectors. Gravure printing can also be used to deposit transparent electrodes made of Ag nanowires.[77] The speed of both the micro-gravure printing roller and web was used to control the formation of the perovskite thin film as well as its thickness. Flexographic printing techniques have been often used on polymer solar cell fabrication to print the transparent electrodes.[66,78,79] Investigations applying flexographic as well as gravure printing techniques to perovskite solar cells are surely in the offing.

Other important techniques employed for the fabrication of perovskite solar cells, even over large areas, are those based on vacuum deposition[13,80] such as chemical vapor deposition (CVD), vapor-assisted sequential processing, vacuum-solid reaction (VSR), and sublimation. As is well known, solar cell metal back electrodes are typically thermally evaporated even when the other layers are solution processed. Additionally, vacuum-assisted techniques also permit the deposition of all the other device layers (ETL, HTL, and perovskite).[19,81–84] Layers deposited in high vacuums can be made to be of highly purity, dense, uniform, scalable, and reproducible.[37,81,84,85] Layer thickness is controlled by deposition rate and time while stoichiometry depends on temperature, pressure, and precursor ratio.[82,84] In general, perovskite vacuum deposition is divided in two different methods: (1) The inorganic layer (PbX_2, X = I, Br, Cl) is coated by a solvent engineering technique and the organic component (e.g., MAI or FAI) is evaporated[14,52,83] and (2) both organic and inorganic components are evaporated.[37,82] Hsiao *et al.*,[37] reported a full vacuum deposited solar cell with PCEs of 15%-17% (0.1 cm^2). The authors determined that device performance depends significantly on the organic halide partial pressure. Fakharuddin *et al.*[52] used vapor-assisted sequential processing to produce a high quality, pin-hole free, and dense perovskite layer on mesoscopic TiO_2 nano-rods for fabricating a module with 8.1% of PCE on an active area of 5.7×5.7 cm^2. According to XRD measurement, the PbI_2 layer was fully converted showing that with the vapor-assisted sequential processing method it was possible to obtain a high purity $CH_3NH_3PbI_3$ layer. Chen *et al.*[86] produced a planar cell with active area of 8×8 cm^2 using VSR. The VSR system consisted of two parallel hot plates which were placed inside a vacuum desiccator. First, a MAI layer solution was sprayed on a hot substrate and dried and a PbI_2 layer was spin coated on a glass/FTO substrate. These were then inserted in a vacuum chamber facing each other and heated at 120 °C and 130 °C, respectively. After evaporation of MAI took place from the top plate, the perovskite layer was formed on the bottom substrate. As a result of the perovskite purity and density reached, cells yielded a PCE of 12.2% and no-hysteresis was reported. The quality of film was determined by optimizing the evaporation time. Leyden *et al.*[81,82,87,88] reported the fabrication of perovskite solar cells and modules using co-evaporation methods in a number of works. Both precursors, $PbCl_2$ and FAI for example, were placed on individual evaporation cells inside a vacuum chamber and a controlled evaporation was carried out. These methods permit either the sequential or simultaneous deposition. The incorporation of FAI induced improvements in the thermal stability of perovskite solar cell while chlorine had a positive effect on efficiency and stability compared with MAI and iodine based analogues, respectively.[81] Cells produced by CVD showed an improvement in efficiency after 42 days and low ageing after 155 days.[87] Devices reached PCEs of 14.2% (1 cm^2)[87] and 9% (12 cm^2).[81] The vacuum methods described above can be implemented over larger areas with appropriate systems.

As mentioned above, the electrodes are generally either deposited by vacuum techniques (more typically) or also by printing techniques. Some groups have instead used lamination processes for applying the top electrode which may be useful for producing either transparent cells or cells on metal foils with efficiencies of 7.6%–13.3%;[89,90] however, currently laminated solar cells evidenced bigger hysteresis than the Au-electrode based analogues and the application over large area modules where patterning is necessary must still be investigated.

In addition to already-available deposition and printing techniques that have been newly applied to the manufacture of perovskite devices, totally new methods have also been devised: Ye *et al.*[91] developed a soft-cover deposition (SCD) technique on large area substrates (51 cm^2). Using the SCD method, the perovskite precursor was spread on a preheated substrate using a polyimide

(PI) film (soft-cover). The PI cover film contained solvent evaporation for a short time (25 s). Once the PI soft cover was removed solvent evaporation and perovskite formation occurred at the same time which yielded a pinhole-free perovskite film with large grain sizes and reduced concentration of grain boundaries in air. The 1 cm^2-area devices showed low hysteresis and high power conversion efficiencies (17.6%). Surface wettability of the soft cover with the precursor solutions, their viscosity, and the thermal crystallization processes were the main parameters governing the formation of the polycrystalline films. Faster crystallization produced material accumulation, showing that the cover must be kept for a few seconds in order to obtain a high quality film. Also a low percentage of perovskite precursor material was wasted (only the 20% of initial amount). Meanwhile, Spyropoulos *et al.*[92] combined an adhesive top electrode and depth-selective laser patterning to fabricate novel two-cell perovskite solar modules. The modules delivered a PCE of 9.75% not so far from 9.80% of small cells, and no-hysteresis.

As a final remark, when upscaling perovskite solar cell technology there are also processing steps that need to be considered which are performed after the deposition of the layers and which also require optimization for large area implementation and in reducing processing times.[19] One of the major post processing steps consists of thermally curing the perovskite precursors as well as the transport layers or electrodes which is usually carried out in hot plates or ovens. Work has started on this front. For example, photonic curing leads to large improvements in the time required to cure the perovskite layers even down to the ms-s range,[93,94] and has also been applied to the TiO_2 layers.[45,95]

CONCLUSION

We have shown that investigations carried out on large area processing of perovskite solar cells and modules provide this technology with huge potential for large scale manufacturing. Already high performance can be reached with low-cost and well-known industrial processes which can optimize the amount of materials used as well as guarantee high throughputs. Solution processing and evaporation or vapor techniques, together with laser processing, have enabled the upscaling of the technology from the initial small laboratory cells to the manufacture of large area modules. More investigations are required to close the efficiency gap which still exists especially when going to the very large areas ($\gg$100 cm^2) compared to small area cells, together with implementing materials/processing strategies that can guarantee long lifetimes. The large area processing techniques we have discussed represent an important manufacturing arsenal for perovskite solar cell technology, which make PSCs ever more interesting not only scientifically but also for investors and commercial exploitation.

ACKNOWLEDGMENTS

This work was supported by the Departamento del Huila's Scholarship Program No. 677 from Huila, Colombia, by MIUR with PRIN 2012 (2012A4Z2RY) "AQUASOL" project, and by Regione Lazio with "Polo Solare Organico" project.

[1] P. Mariani, L. Vesce, and A. Di Carlo, Semicond. Sci. Technol. **30**, 104003 (2015).
[2] A. Fakharuddin, R. Jose, T. M. Brown, F. Fabregat-Santiago, and J. Bisquert, Energy Environ. Sci. **7**, 3952 (2014).
[3] F. C. Krebs, Sol. Energy Mater. Sol. Cells **93**, 465 (2009).
[4] Y. Han, S. Meyer, Y. Dkhissi, K. Weber, J. M. Pringle, U. Bach, L. Spiccia, and Y.-B. Cheng, J. Mater. Chem. A **3**, 8139 (2015).
[5] Y. Rong, Z. Ku, A. Mei, T. Liu, M. Xu, S. Ko, X. Li, and H. Han, J. Phys. Chem. Lett. **5**, 2160 (2014).
[6] X. Li, M. Tschumi, H. Han, S. S. Babkair, R. A. Alzubaydi, A. A. Ansari, S. S. Habib, M. K. Nazeeruddin, S. M. Zakeeruddin, and M. Grätzel, Energy Technol. **3**, 551 (2015).
[7] F. Matteocci, S. Casaluci, S. Razza, A. Guidobaldi, T. M. Brown, A. Reale, and A. Di Carlo, J. Power Sources **246**, 361 (2014).
[8] F. Giordano, A. Guidobaldi, E. Petrolati, L. Vesce, R. Riccitelli, A. Reale, T. M. Brown, and A. Di Carlo, Prog. Photovoltaics Res. Appl. **21**, 1653 (2013).
[9] H. Hoppe, M. Seeland, and B. Muhsin, Sol. Energy Mater. Sol. Cells **97**, 119 (2012).
[10] Y. Galagan, E. W. C. Coenen, W. Verhees, and R. Andriessen, J. Mater. Chem. A **4**, 5700 (2016).
[11] G. Mincuzzi, A. L. Palma, A. Di Carlo, and T. M. Brown, Chemelectrochem **3**, 9 (2016).
[12] C.-W. Chen, H.-W. Kang, S.-Y. Hsiao, P.-F. Yang, K.-M. Chiang, and H.-W. Lin, Adv. Mater. **26**, 6647 (2014).

[13] M. Liu, M. B. Johnston, and H. J. Snaith, Nature **501**, 395 (2013).
[14] S. Casaluci, L. Cinà, A. Pockett, P. S. Kubiak, R. G. Niemann, A. Reale, A. Di Carlo, and P. J. Cameron, J. Power Sources **297**, 504 (2015).
[15] National Renewable Enery Laboratory, 2016, http://www.nrel.gov/ncpv/images/efficiency_chart.jpg.
[16] W. Chen, Y. Wu, Y. Yue, J. Liu, W. Zhang, X. Yang, H. Chen, E. Bi, I. Ashraful, M. Gratzel, and L. Han, Science **350**, 944 (2015).
[17] M. Yang, Y. Zhou, Y. Zeng, C.-S. Jiang, N. P. Padture, and K. Zhu, Adv. Mater. **27**, 6363 (2015).
[18] M. A. Green, K. Emery, Y. Hishikawa, W. Warta, and E. D. Dunlop, Prog. Photovoltaics Res. Appl. **24**, 3 (2016).
[19] X. Li, D. Bi, C. Yi, J.-D. Decoppet, J. Luo, S. M. Zakeeruddin, A. Hagfeldt, and M. Gratzel, Science **353**(6294), 58 (2016).
[20] F. Matteocci, S. Razza, F. Di Giacomo, S. Casaluci, G. Mincuzzi, T. M. Brown, A. D'Epifanio, S. Licoccia, and A. Di Carlo, Phys. Chem. Chem. Phys. **16**, 3918 (2014).
[21] W. Qiu, T. Merckx, M. Jaysankar, C. Masse de la Huerta, L. Rakocevic, W. Zhang, U. W. Paetzold, R. Gehlhaar, L. Froyen, J. Poortmans, D. Cheyns, H. J. Snaith, and P. Heremans, Energy Environ. Sci. **9**, 484 (2016).
[22] F. Matteocci, L. Cinà, F. Di Giacomo, S. Razza, A. L. Palma, A. Guidobaldi, A. D'Epifanio, S. Licoccia, T. M. Brown, A. Reale, and A. Di Carlo, Prog. Photovoltaics Res. Appl. **24**, 436 (2014).
[23] J. H. Heo, H. J. Han, D. Kim, T. K. Ahn, and S. H. Im, Energy Environ. Sci. **8**, 1602 (2015).
[24] J. Burschka, N. Pellet, S.-J. Moon, R. Humphry-Baker, P. Gao, M. K. Nazeeruddin, and M. Grätzel, Nature **499**, 316 (2013).
[25] A. T. Mallajosyula, K. Fernando, S. Bhatt, A. Singh, B. W. Alphenaar, J.-C. Blancon, W. Nie, G. Gupta, and A. D. Mohite, Appl. Mater. Today **3**, 96 (2016).
[26] S. Razza, F. Di Giacomo, F. Matteocci, L. Cinà, A. L. Palma, S. Casaluci, P. Cameron, A. D'Epifanio, S. Licoccia, A. Reale, T. M. Brown, and A. Di Carlo, J. Power Sources **277**, 286 (2015).
[27] S. Razza, F. Matteocci, F. Di Giacomo, M. Dianetti, A. L. Palma, F. Brunetti, T. M. Brown, and A. Di Carlo, in *HOPV Conference*, 2015.
[28] J. H. Kim, S. T. Williams, N. Cho, C.-C. Chueh, and A. K.-Y. Jen, Adv. Energy Mater. **5**, 1401229 (2015).
[29] Z. Yang, C.-C. Chueh, F. Zuo, J. H. Kim, P.-W. Liang, and A. K.-Y. Jen, Adv. Energy Mater. **5**, 1500328 (2015).
[30] D. Vak, K. Hwang, A. Faulks, Y. S. Jung, N. Clark, D. Y. Kim, G. J. Wilson, and S. E. Watkins, Adv. Energy Mater. **5**, 1 (2015).
[31] K. Hwang, Y. S. Jung, Y. J. Heo, F. H. Scholes, S. E. Watkins, J. Subbiah, D. J. Jones, D. Y. Kim, and D. Vak, Adv. Mater. **27**, 1241 (2015).
[32] Solliance, 2016, http://www.solliance.eu/news/item/?tx_ttnews%5Btt_news%5D=374&cHash=9cca0703becbdfb276110aa258244a5e Press release.
[33] A. Reale, L. La Notte, L. Salamandra, G. Polino, G. Susanna, T. M. Brown, F. Brunetti, and A. Di Carlo, Energy Technol. **3**, 385 (2015).
[34] Z. Liang, S. Zhang, X. Xu, N. Wang, J. Wang, X. Wang, Z. Bi, G. Xu, N. Yuan, and J. Ding, RSC Adv. **5**, 60562 (2015).
[35] A. Barrows, A. Pearson, C. Kwak, A. Dunbar, A. Buckley, and D. Lidzey, Energy Environ. Sci. **7**, 1 (2014).
[36] S. Das, B. Yang, G. Gu, P. C. Joshi, I. N. Ivanov, C. M. Rouleau, T. Aytug, D. B. Geohegan, and K. Xiao, ACS Photonics **2**, 680 (2015).
[37] S.-Y. Hsiao, H.-L. Lin, W.-H. Lee, W.-L. Tsai, K.-M. Chiang, W.-Y. Liao, C.-Z. Ren-Wu, C.-Y. Chen, and H.-W. Lin, Adv. Mater. **28**, 7013 (2016).
[38] K. M. Boopathi, M. Ramesh, P. Perumal, Y.-C. Huang, C.-S. Tsao, Y.-F. Chen, C.-H. Lee, and C.-W. Chu, J. Mater. Chem. A **3**, 9257 (2015).
[39] Y.-S. Jung, K. Hwang, F. H. Scholes, S. E. Watkins, D.-Y. Kim, and D. Vak, Sci. Rep. **6**, 20357 (2016).
[40] F. Li, C. Bao, H. Gao, W. Zhu, T. Yu, J. Yang, G. Fu, X. Zhou, and Z. Zou, Mater. Lett. **157**, 38 (2015).
[41] F. Shao, L. Xu, Z. Tian, Y. Xie, Y. Wang, P. Sheng, D. Wang, and F. Huang, RSC Adv. **6**, 42377 (2016).
[42] S. Casaluci, M. Gemmi, V. Pellegrini, A. Di Carlo, and F. Bonaccorso, Nanoscale **8**, 5368 (2016).
[43] A. L. Palma, L. Cinà, S. Pescetelli, A. Agresti, M. Raggio, R. Paolesse, F. Bonaccorso, and A. Di Carlo, Nano Energy **22**, 349 (2016).
[44] M. Dianetti, F. Di Giacomo, G. Polino, C. Ciceroni, A. Liscio, A. D'Epifanio, S. Licoccia, T. M. Brown, A. Di Carlo, and F. Brunetti, Sol. Energy Mater. Sol. Cells **140**, 150 (2015).
[45] F. Di Giacomo, V. Zardetto, A. D'Epifanio, S. Pescetelli, F. Matteocci, S. Razza, A. Di Carlo, S. Licoccia, W. M. M. Kessels, M. Creatore, and T. M. Brown, Adv. Energy Mater. **5**, 1401808 (2015).
[46] L. Zhang, T. Liu, L. Liu, M. Hu, Y. Yang, A. Mei, and H. Han, J. Mater. Chem. A **3**, 9165 (2015).
[47] Z. Ku, Y. Rong, M. Xu, T. Liu, and H. Han, Sci. Rep. **3**, 3132 (2013).
[48] A. Mei, X. Li, L. Liu, Z. Ku, T. Liu, Y. Rong, M. Xu, M. Hu, J. Chen, Y. Yang, M. Gratzel, and H. Han, Science **345**, 295 (2014).
[49] K. Cao, Z. Zuo, J. Cui, Y. Shen, T. Moehl, S. M. Zakeeruddin, M. Grätzel, and M. Wang, Nano Energy **17**, 171 (2015).
[50] X. Xu, Z. Liu, Z. Zuo, M. Zhang, Z. Zhao, Y. Shen, H. Zhou, Q. Chen, Y. Yang, and M. Wang, Nano Lett. **15**, 2402 (2015).
[51] A. Fakharuddin, F. Di Giacomo, A. L. Palma, F. Matteocci, I. Ahmed, S. Razza, A. D'Epifanio, S. Licoccia, J. Ismail, A. Di Carlo, T. M. Brown, and R. Jose, ACS Nano **9**, 8420 (2015).
[52] A. Fakharuddin, A. L. Palma, F. Di Giacomo, S. Casaluci, F. Matteocci, Q. Wali, M. Rauf, A. Di Carlo, T. M. Brown, and R. Jose, Nanotechnology **26**, 494002 (2015).
[53] S.-J. Moon, J.-H. Yum, L. Lofgren, A. Walter, L. Sansonnens, M. Benkhaira, S. Nicolay, J. Bailat, and C. Ballif, IEEE J. Photovoltaics **5**, 1087 (2015).
[54] R. Gehlhaar, T. Merckx, C. M. de la Huerta, W. Qiu, D. Cheyns, and T. Aernouts, SPIE Newsroom (29 October 2015).
[55] Y. Galagan, H. Fledderus, H. Gorter, H. H. 't Mannetje, S. Shanmugam, R. Mandamparambil, J. Bosman, J.-E. J. M. Rubingh, J.-P. Teunissen, A. Salem, I. G. de Vries, R. Andriessen, and W. A. Groen, Energy Technol. **3**, 834 (2015).
[56] R. Søndergaard, M. Hösel, D. Angmo, T. T. Larsen-Olsen, and F. C. Krebs, Mater. Today **15**, 36 (2012).
[57] B. Susrutha, L. Giribabu, and S. P. Singh, Chem. Commun. **51**, 14696 (2015).

[58] S. A. Gevorgyan, M. V. Madsen, H. F. Dam, M. Jørgensen, C. J. Fell, K. F. Anderson, B. C. Duck, A. Mescheloff, E. A. Katz, A. Elschner, R. Roesch, H. Hoppe, M. Hermenau, M. Riede, and F. C. Krebs, Sol. Energy Mater. Sol. Cells **116**, 187 (2013).
[59] F. C. Krebs, T. Tromholt, and M. Jørgensen, Nanoscale **2**, 873 (2010).
[60] R. Rösch, F. C. Krebs, D. M. Tanenbaum, and H. Hoppe, Sol. Energy Mater. Sol. Cells **97**, 176 (2012).
[61] T. M. Brown, F. De Rossi, F. Di Giacomo, G. Mincuzzi, V. Zardetto, A. Reale, and A. Di Carlo, J. Mater. Chem. A **2**, 10788 (2014).
[62] Z. Wei, H. Chen, K. Yan, and S. Yang, Angew. Chem., Int. Ed. **53**, 13239 (2014).
[63] K. Shin, J. Park, and C. Lee, Thin Solid Films **598**, 95 (2016).
[64] T. M. Schmidt, T. T. Larsen-Olsen, J. E. Carlé, D. Angmo, and F. C. Krebs, Adv. Energy Mater. **5**, 1500569 (2015).
[65] V. Shrotriya, Solarmer, Printed Electronics USA 15, 2010, http//www.slideshare.net/vshrotriya/organic-Solar-Cells.
[66] M. Hösel, R. R. Søndergaard, M. Jørgensen, and F. C. Krebs, Energy Technol. **1**, 102 (2013).
[67] D. Kaduwal, H. Schleiermacher, J. Schulz-Gericke, S. Schiefer, Y. Liang Tan, J. Zhang, B. Zimmermann, and U. Würfel, Sol. Energy Mater. Sol. Cells **136**, 200 (2015).
[68] T. R. Andersen, H. F. Dam, M. Hösel, M. Helgesen, J. E. Carle, T. T. Larsen-Olsen, S. A. Gevorgyan, J. W. Andreasen, J. Adams, N. Li, F. Machui, G. D. Spyropoulos, T. Ameri, N. Lemaitre, M. Legros, A. Scheel, D. Gaiser, K. Kreul, S. Berny, O. R. Lozman, S. Nordman, M. Valimaki, M. Vilkman, R. R. Sondergaard, M. Jorgensen, C. J. Brabec, and F. C. Krebs, Energy Environ. Sci. **7**, 2925 (2014).
[69] F. Di Giacomo, A. Fakharuddin, R. Jose, and T. M. Brown, "Progress, challenges and perspectives in flexible perovskite solar cells," Energy Environ. Sci. (published online, 2016).
[70] Y. Galagan and R. Andriesse, "Organic photvoltaics: Technologies and manufacturing," in *Third Gener. Photovoltaics*, edited by V. Fthenakis (InTech, 2012), Chap. 3.
[71] D. Angmo, T. T. Larsen-Olsen, M. Jørgensen, R. R. Søndergaard, and F. C. Krebs, Adv. Energy Mater. **3**, 172 (2013).
[72] S.-G. Li, K.-J. Jiang, M.-J. Su, X.-P. Cui, J.-H. Huang, Q.-Q. Zhang, X.-Q. Zhou, L.-M. Yang, and Y.-L. Song, J. Mater. Chem. A **3**, 9092 (2015).
[73] M. Bag, Z. Jiang, L. A. Renna, S. P. Jeong, V. M. Rotello, and D. Venkataraman, Mater. Lett. **164**, 472 (2016).
[74] M. Hosseini Zori and A. Soleimani-Gorgani, J. Eur. Ceram. Soc. **32**, 4271 (2012).
[75] M. M. Voigt, R. C. I. Mackenzie, S. P. King, C. P. Yau, P. Atienzar, J. Dane, P. E. Keivanidis, I. Zadrazil, D. D. C. Bradley, and J. Nelson, Sol. Energy Mater. Sol. Cells **105**, 77 (2012).
[76] Q. Hu, H. Wu, J. Sun, D. Yan, Y. Gao, and J. Yang, Nanoscale **8**, 5350 (2016).
[77] W. J. Scheideler, J. Smith, I. Deckman, S. Chung, A. C. Arias, and V. Subramanian, J. Mater. Chem. C **4**, 3248 (2016).
[78] D. Angmo and F. C. Krebs, J. Appl. Polym. Sci. **129**, 1 (2013).
[79] F. C. Krebs, J. Fyenbo, and M. Jørgensen, J. Mater. Chem. **20**, 8994 (2010).
[80] Q. Chen, H. Zhou, Z. Hong, S. Luo, H.-S. Duan, H.-H. Wang, Y. Liu, G. Li, and Y. Yang, J. Am. Chem. Soc. **136**, 622 (2014).
[81] M. R. Leyden, Y. Jiang, and Y. Qi, J. Mater. Chem. A **4**, 13125 (2016).
[82] L. K. Ono, M. R. Leyden, S. Wang, and Y. Qi, J. Mater. Chem. A **4**, 6693 (2016).
[83] L. Gouda, R. Gottesman, S. Tirosh, E. Haltzi, J. Hu, A. Ginsburg, D. A. Keller, Y. Bouhadana, and A. Zaban, Nanoscale **8**, 6386 (2016).
[84] Q. Guo, C. Li, W. Qiao, S. Ma, F. Wang, B. Zhang, L. Hu, S. Dai, and Z. Tan, Energy Environ. Sci. **9**, 1486 (2016).
[85] T. P. Gujar and M. Thelakkat, Energy Technol. **4**, 449 (2016).
[86] X. Chen, H. Cao, H. Yu, H. Zhu, H. Zhou, L. Yang, and S. Yin, J. Mater. Chem. A **4**, 9124 (2016).
[87] M. R. Leyden, M. V. Lee, S. R. Raga, and Y. Qi, J. Mater. Chem. A **3**, 16097 (2015).
[88] M. R. Leyden, L. K. Ono, S. R. Raga, Y. Kato, S. Wang, and Y. Qi, J. Mater. Chem. A **2**, 18742 (2014).
[89] D. Bryant, P. Greenwood, J. Troughton, M. Wijdekop, M. Carnie, M. Davies, K. Wojciechowski, H. J. Snaith, T. Watson, and D. Worsley, Adv. Mater. **26**, 7499 (2014).
[90] M. Makha, S. L. Fernandes, S. Jenatsch, T. Offermans, J. Schleuniger, J.-N. Tisserant, A. C. Véron, and R. Hany, Sci. Technol. Adv. Mater. **17**, 260 (2016).
[91] F. Ye, H. Chen, F. Xie, W. Tang, M. Yin, J. He, E. Bi, Y. Wang, X. Yang, and L. Han, Energy Environ. Sci. **9**, 2295 (2016).
[92] G. D. Spyropoulos, C. O. Ramirez Quiroz, M. Salvador, Y. Hou, N. Gasparini, P. Schweizer, J. Adams, P. Kubis, N. Li, E. Spiecker, T. Ameri, H. Egelhaaf, and C. J. Brabec, Energy Environ. Sci. **9**, 2302 (2016).
[93] J. Troughton, C. Charbonneau, M. J. Carnie, M. L. Davies, D. A. Worsley, and T. M. Watson, J. Mater. Chem. A **3**, 9123 (2015).
[94] J. Troughton, M. J. Carnie, M. L. Davies, C. Charbonneau, E. Jewell, D. A. Worsley, and T. M. Watson, J. Mater. Chem. A **4**, 3471 (2016).
[95] S. Das, G. Gu, P. C. Joshi, B. Yang, T. Aytug, C. M. Rouleau, D. B. Geohegan, and K. Xiao, J. Mater. Chem. A **4**, 9685 (2016).
[96] F. C. Krebs, M. Jørgensen, K. Norrman, O. Hagemann, J. Alstrup, T. D. Nielsen, J. Fyenbo, K. Larsen, and J. Kristensen, Sol. Energy Mater. Sol. Cells **93**, 422 (2009).
[97] C. J. Brabec, U. Scherf, V. A. D'iakonov, and D. Angmo, *Organic Photovoltaics: Materials Device Physics Manufacturing Technologies* (Wiley-VCH Verlag GmbH & Co. KGaA, Weinheim, Germany, 2008).
[98] *Printed Organic Molecular Electronics*, edited by D. Gamota, P. Brazis, K. Kalyanasundaram, and J. Zhang (Springer, US, Boston, MA, 2004).
[99] Solaronix SA, personal communication and 11th July 2016 press release, https://www.solaronix.com/news/solaronix-achieves-major-breakthrough-toward-perovskite-solar-cell-industrialization/.